Scanned perturbation technique for imaging electromagnetic standing wave patterns of microwave cavities

Ali Gokirmak, Dong-Ho Wu, J. S. A. Bridgewater, and Steven M. Anlage[a)]
Center for Superconductivity Research, Department of Physics, University of Maryland, College Park, Maryland 20742-4111

(Received 7 May 1998; accepted for publication 2 June 1998)

We have developed a method to measure the electric field standing wave distributions in a microwave resonator using a scanned perturbation technique. Fast and reliable solutions to the Helmholtz equation (and to the Schrödinger equation for two-dimensional systems) with arbitrarily shaped boundaries are obtained. We use a pin perturbation to image primarily the microwave electric field amplitude, and we demonstrate the ability to image broken time-reversal symmetry standing wave patterns produced with a magnetized ferrite in the cavity. The whole cavity, including areas very close to the walls, can be imaged using this technique with high spatial resolution over a broad range of frequencies. © *1998 American Institute of Physics.* [S0034-6748(98)00909-5]

I. INTRODUCTION

Quantitative mapping of the electromagnetic fields inside a metallic cavity is important for various technological and scientific reasons. An experimental understanding of the behavior of electromagnetic waves in irregularly shaped structures is important for the design of electrical circuits, particularly those housed inside metallic containers which are susceptible to strong concentrations of electromagnetic fields. The degree of concentration of the field depends sensitively on the operating frequency and shape of the device. Of more scientific interest, electromagnetic resonators can be used to represent quantum mechanical potential wells. In this case, the standing wave patterns can reveal the probability density of the corresponding solution to the Schrödinger equation for an infinite square well potential of arbitrary shape. These eigenfunctions are important for understanding the behavior of mesoscopic structures, and will be crucial for the design of nanoscale electronic devices. In addition, a great deal of interesting physics can be explored by means of an experimental understanding of the behavior of the wave functions in irregular shaped devices, including wave localization and wave function fluctuations. To investigate the wave functions, one needs a simple and reliable method of imaging electromagnetic waves in cavities. In this article we present a simple method to image the standing wave eigenfunctions of two-dimensional electromagnetic cavities and their corresponding quantum eigenfunctions.

Imaging of electromagnetic standing waves in microwave resonators was pioneered by Slater and co-workers.[1] They used the technique of cavity perturbation to selectively measure the microwave electric and magnetic field amplitudes using a scanned perturbation. Others have refined this technique by modulating the perturbation to measure both electric and magnetic fields.[2] More recently, forms of near-field ''microwave microscopy'' have been developed to probe electromagnetic fields on small length scales (much less than the free space wavelength of the radiation) in resonant[3] and nonresonant[4–6] devices. Other recent derivatives of Slater's work have examined the standing wave patterns of electromagnetic resonators which simulate wave chaotic systems in two dimensions.[7–10] In several of the techniques mentioned above, one measures a mixture of electric and magnetic fields, and some methods are not easily scaled to high frequency imaging. Further, none of these methods has demonstrated the ability to image eigenfunctions in the absence of time-reversal symmetry, which is an important consequence of device performance under magnetic field. We have developed an experimental method of imaging primarily the microwave electric field amplitude which operates over a very broad range of frequencies with or without time-reversal symmetry. In this article we describe the experimental method along with our experimental results obtained from quasi-two-dimensional cavities, both integrable and nonintegrable. The method can be used to test fundamental wave dynamics in an irregularly shaped structure, and also can be used for performance tests of cavity-based microwave devices.

For the investigation of fundamental wave (or quantum) mechanical behavior, one exploits the electromagnetic analog[11,12] of the Schrödinger equation in two dimensions (2D). Both the time-independent Schrödinger equation and the Helmholtz equation are linear second order differential equations with respect to space with constant coefficients:

$$\nabla^2\Psi_n + 2m(\epsilon_n - V)/\hbar^2\Psi_n = 0, \tag{1}$$

$$\nabla^2 E_{zi} + k_i^2 E_{zi} = 0. \tag{2}$$

The Schrödinger equation, Eq. (1), describes the nth excited eigenfunction Ψ_n of a particle of mass m in a potential V, where ϵ_n is the energy of the nth excited state, and $\hbar$ is Planck's constant divided by 2π. In the Helmholtz equation, Eq. (2), E_{zi} is the z component of the electric field, and k_i is the wave vector in the propagation direction of the ith mode (it is assumed that the resonator is much smaller in the z direction than in the x and y directions). In general k_i^2

[a)]Electronic mail: anlage@squid.umd.edu;http://www.csr.umd.edu/

$=\omega_i^2\mu\epsilon$, where ω_i is the ith resonant frequency of the cavity with uniform permittivity ε and permeability μ. The probability density $|\Psi_n|^2$ in the Schrödinger equation for the quantum mechanical problem is analogous to $|E_{zi}|^2$ in the Helmholtz equation for the electromagnetic problem, as long as the $2m(\epsilon_n-V)/\hbar^2$ and k_i^2 terms in these equations are constant. In a thin microwave cavity where E_z is uniform in the z direction, the solutions to the Helmholtz equation with perfectly conducting walls ($E_{zi}=0$ at the boundary) are equivalent to the solutions of the two-dimensional Schrödinger equation with hard wall boundaries ($\Psi_n = 0$ at the boundary) of the same geometry.

The experimental technique we developed uses a perturbation to obtain a spatially resolved measure of $|E_{zi}|^2$ in a hollow microwave cavity. At the same time, the technique allows us to measure the analogous quantum eigenfunctions of 2D infinite square well potentials. We can use this method to study the properties of any 2D quantum dot where the solution to the Schrödinger equation is needed, and analog solutions for the eigenvalues and eigenfunctions can be obtained.

The outline for the rest of the article is as follows. In Sec. II we discuss the principle of the measurement in detail, while in Sec. III we describe the experimental setup. In Sec. IV we show some sample data, and discuss thier general features and make comparisons with theory. The limitations and constraints of the technique are discussed in Sec. V, while in Sec. VI we summarize our findings.

II. PRINCIPLE OF THE MEASUREMENT

When microwave electromagnetic fields in a cavity are perturbed, the resonant frequency ω is altered as[1]

$$\omega^2=\omega_0^2\left(1+\int (B^2-E^2)dV_p\right), \tag{3}$$

where ω_0 is the resonant frequency of the unperturbed cavity, B is the microwave magnetic field and E is the microwave electric field at the location of the perturbation. The integral is taken over the perturbation volume V_p. The field components in the expression are normalized over the volume of the cavity such that $\int E^2dV=1$, $\int B^2dV=1$. If we change the location of a metallic perturbation in the cavity and record the resonant frequency for each point, we can image a combination of E^2 and B^2 inside the cavity. Note that while the contribution of E^2 results in a frequency shift to a lower frequency (due to the negative sign in front of E^2) the contribution of B^2 results in a shift to a higher frequency. Throughout the development of our experimental technique, we find that the shape of the perturbation determines the relative contribution of E^2 and B^2 to the shift in the resonant frequency.

Both pins and spheres are used as perturbations in the measurements presented here. Spheres introduce significant contributions to the frequency shift from the magnetic field components. In our measurements we want to image only $|E_z|^2$ in the cavity, hence pin perturbations are used to minimize the magnetic field contribution.

The electromagnetic modes of a two-dimensional microwave cavity are particularly simple, as there are only three

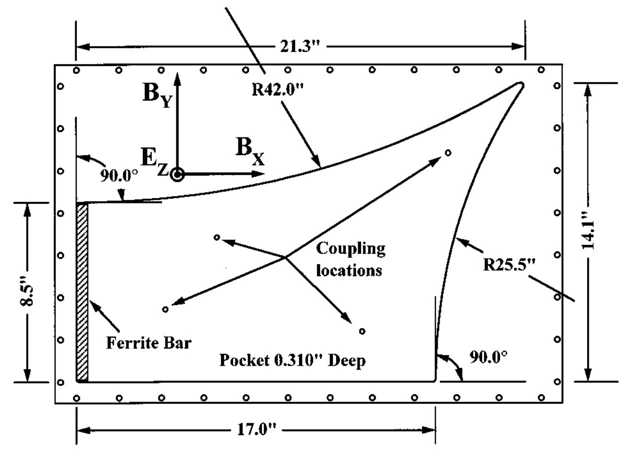

FIG. 1. Diagram of the quarter bowtie resonator. The resonator is formed by a 0.310 in. deep pocket in the solid brass piece. For some experiments, a ferrite bar is located on the left-hand wall. The axes show the three components of the electromagnetic fields in transverse magnetic modes of thin microwave resonators.

nonzero components of the electromagnetic field. A 2D cavity is designed to have a height (z) significantly smaller than the dimensions in the horizontal plane (x, y) so that there is no wave vector component in the z direction below a well-defined cutoff frequency. For our cavities with a height of 0.310 in., below 19.05 GHz only 2D transverse magnetic (TM) modes can propagate, hence only E_z, B_x, and B_y can have nonzero values (see Fig. 1). There are approximately 1000 TM modes below 19.05 GHz in the quarter bowtie cavity discussed below (Fig. 1).[13]

III. EXPERIMENTAL SETUP

As shown in Fig. 2, the cavity is imaged using a microwave vector network analyzer and a two-dimensional scanner which moves a small metallic perturbation inside the cavity through the influence of an external magnetic field. The perturbation can be inserted and removed through a small coupling hole on the cavity lid so that the cavity does not have to be opened each time the perturbation is changed. In the rest of Sec. III we shall discuss the types of microwave cavities we have imaged, the microwave system for the measurement, the perturbation scanner and the perturbations themselves.

A. Cavity

In our experiment, a classically chaotic two-dimensional potential well is used. Four intersecting circles with radii

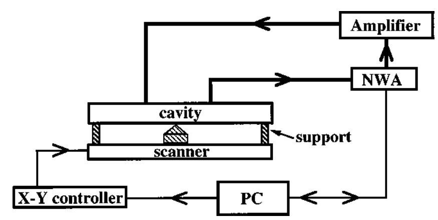

FIG. 2. Schematic diagram of the experiment. Thick lines represent microwave signal paths, while the thinner lines represent low frequency control and data signal paths.

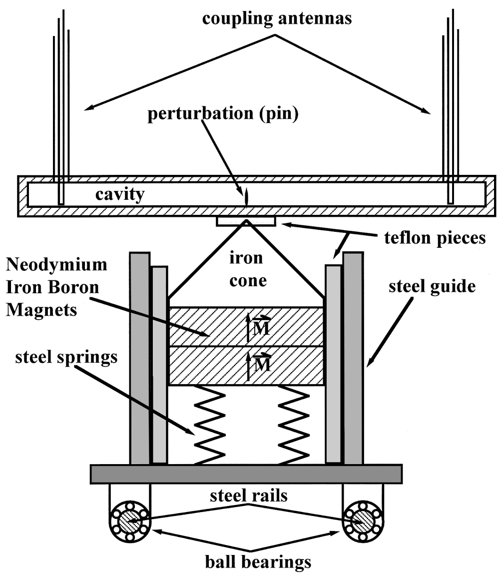

FIG. 3. Closeup schematic view of magnet ensemble and pin pertubation inside the microwave cavity. Also shown are the coupling antennas in the cavity.

smaller than the separation between the centers form a closed region resembling a bowtie. The system we use in our experiments is one quarter of this region (see Fig. 1). This geometry ensures that all typical ray-trajectory orbits are chaotic and all periodic orbits are isolated,[13,14] and allows one to study the eigenmodes of wave chaotic systems.[15]

The quarter bowtie is carved into brass and the surface is plated with copper to reduce the surface resistance and increase the quality factor of the cavity modes. A copper-plated flat lid closes the cavity from the top. There are four holes on the lid where the coupling probes are inserted into the cavity. The quality factor (Q) for the bowtie cavity range from 700 to 3000, depending upon the resonance.

A second rectangular cavity was used for measurements in a simple geometry to check the validity of our experimental technique. The dimensions of the rectangular cavity are 7.5 in.$\times$14.0 in.$\times$0.310 in. high.

B. Vector network analyzer and the microwave setup

An HP8722D vector network analyzer (NWA) was used to measure the resonant frequency of the cavity for each position of the perturbation. A signal coming out of the network analyzer is amplified by an HP8349B microwave amplifier (see Fig. 2). The output of the amplifier is injected into the cavity through an E-plane coupling probe, and the transmitted signal from the cavity is picked up by a second E-plane coupling probe (see Figs. 2 and 3). The coupling probes are made out of semirigid coaxial cable by stripping the outer conductor off one end, with the length of the exposed inner conductor slightly less than the cavity height. The coupling probes are connected to the top lid of the cavity with adjustable micrometers and are isolated electrically from the cavity. The signal picked up by the second coupling probe is taken to the detector of the network analyzer. The resonant frequencies of the cavity correspond to local maxima in the transmission amplitude between the two ports of the network analyzer in the frequency domain.

C. Scanning setup

A two-dimensional scanner[16] carrying a magnet ensemble under the cavity is used to move a perturbation inside the cavity to map out the electric field. The ensemble is composed of two magnets and a magnet iron cone on top (see Fig. 3). To produce an isotropic and strong restoring force on the steel perturbation inside the cavity, the field from the magnets is focused by the magnet iron cone. The platform is moved on steel rails by means of belts driven by stepper motors. In order to image the fine details of high frequency eigenmodes, we redesigned the scanner to have as little static and dynamic friction as possible between the carriage and the rails supporting it. This significantly increased the accuracy in the magnet location compared to the original design of the scanner.

Further, to reduce friction and keep the magnet ensemble at a constant separation from the cavity, a thin Teflon piece was inserted between the cone tip and the cavity. The magnet and cone combination is supported by four springs glued onto the mobile platform. The magnets and cone are placed inside a square case and are free to move up and down to follow the small changes in the scanner-cavity separation. The case is made out of steel in order to concentrate the return magnetic flux from the cone. This minimizes the effect of the scanning magnets on magnetically sensitive objects in or around the cavity, which are unrelated to the perturbation (e.g., a ferrite bar introduced into the cavity for some of the measurements).

D. Data acquisition

A computer controls both the network analyzer and the scanner and records the data transferred from the network analyzer. The network analyzer measures the transmission magnitude through the cavity and is set to take data at 1601 frequency points per span, with a typical span of 3 MHz centered on one of the resonant modes. Data points on the network analyzer are smoothed to reduce the noise level in the data. The resonant peak is followed as the perturbation is moved, and the frequency corresponding to the maximum transmission amplitude is recorded at each stationary position of the perturbation. The perturbation is moved on a square grid with step sizes ranging from 0.2 to 0.05 in., depending on the frequency of the mode to be imaged (there are 71 600 data points on the images made with a step size of 0.05 in.). For most of the perturbations, we observed that the maximum shift in resonant frequency due to the perturbation is on the order of 10 MHz. To test the resolution for frequency shift, we examined a rectangular cavity eigenmode of resonant frequency 1.5 GHz. The 3 dB bandwidth of this mode was 6.5 MHz (the quality factor of this mode is 1250) and we could reliably distinguish a shift on the order of 5 kHz. Thus we are able to distinguish changes in the resonant frequency of about one part in 10^3 of the 3 dB bandwidth.

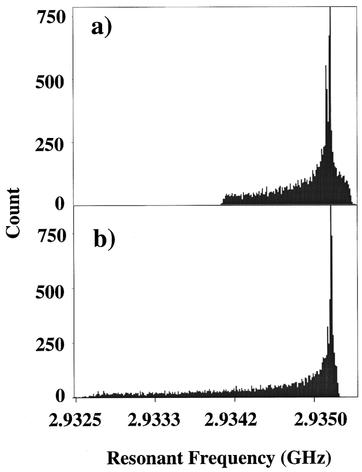

FIG. 4. Distribution of frequency shifts for (a) spherical perturbation and (b) pin perturbation in the resonant mode of a thin rectangular cavity shown in Figs. 5 and 6.

E. Perturbation

In the development of this technique, we have tried various sizes of metallic pins and spheres to find the optimum perturbation. Experiments indicate that the perturbation can be significantly smaller than the wavelength of the radiation and still produce excellent images. A perturbation introduced into the cavity shifts the resonant frequency of the cavity by an amount proportional to a combination of the electric and magnetic field amplitudes at the location of perturbation. For a spherical metallic perturbation, the magnetic field contribution to the shift in the resonant frequency is half of the contribution of the electric field:[1]

$$\frac{\omega^2-\omega_0^2}{\omega_0^2}=3\left(\frac{4\pi}{3}r_0^3\right)\left(\frac{1}{2}B_0^2-E_0^2\right), \tag{4}$$

where r_0 is the radius of the spherical perturbation, E_0 is the averaged electric field, B_0 is the averaged magnetic field, each being separately normalized and averaged over the volume of the perturbation. The spectrum of frequency shifts for a spherical perturbation (radius of 1/16 in.) in a rectangular cavity eigenmode shows the expected distribution [Fig. 4(a)]. Approximately 30% of the frequency shift data turns out to be higher than the resonant frequency of the empty cavity. These are the points where the magnetic field contribution dominates the electric field contribution. However, the negative frequency shift is, at least partially, reduced by the magnetic field contribution. For our purposes this is unacceptable because we want to image only $|E_z|^2$.

To meet the goal of imaging electric field in the cavity, we use a pin with rounded ends to scan inside the cavity. The spectrum of frequency shifts produced by a pin perturbation is shown in Fig. 4(b). Since most of the resonant frequencies are below the unperturbed resonant frequency, it is clear that the pin measures mainly the electric fields in the cavity. For frequencies below 9 GHz, we use a pin whose body has a diameter of 0.0220 in. and height of 0.2430 in. For frequencies higher than 9 GHz we use a smaller pin with a cylindrical body 0.0085 in. in diameter and 0.1535 in. in height. Experimentally, we observe about a 10% contribution from the magnetic field components for these pins [Fig. 4(b)].

F. Imaging with a magnetized ferrite in the cavity

It is of interest to investigate the eigenvalues and eigenfunctions of chaotic quantum systems with and without time reversal symmetry.[10,13] By introducing a ferrite into the cavity and magnetizing it, one can add a nonreciprocal phase shift to the electromagnetic waves in the cavity, and thus break time-reversal symmetry.[10,13,17] The off-diagonal terms in the ferrite permeability tensor induce a phase shift for reflected waves off the ferrite which changes magnitude significantly when the time evolution of the wave is reversed. However, due to the complex nature of ferrite electrodynamics, the amount of this nonreciprocal phase shift is strongly frequency dependent,[17] and only becomes large enough to fully break time-reversal symmetry in a frequency window above 13.5 GHz for the cavity shown in Fig. 1. Hence it is imperative to image eigenfunctions up to the highest frequencies possible to see the effects of time-reversal symmetry breaking on the wave chaotic eigenfunctions.

The ferrite used in the measurements[18] is 0.2 in. thick, 0.310 in. high, and 8.4 in. long. It is placed adjacent to the short linear boundary on the left side of Fig. 1. The ferrite is magnetized with ten 2 in.×2 in.×0.5 in. magnets placed outside the cavity. The magnets are placed over and under the cavity, centered on the ferrite in two linear arrays. These magnets provide a uniform dc magnetic field in the *z* direction. The magnets are held in place with a *C*-shaped steel piece, which concentrates the return magnetic field flux and minimizes the effect of these stationary magnets on the perturbation scanned inside the cavity. Similarly the scanner magnet is placed in a steel holder concentrating the field and minimizing the effect of the scanning magnet on the ferrite. Although the effect of the scanner magnet is reduced significantly with the steel holder, there still is a visible change in the resonant frequency of the cavity as a function of the scanner magnet location not caused by the perturbation. This undesired effect is significantly reduced by subtracting a background from the eigenmode image (see Sec. IV C).

IV. DATA

A. Comparison between theory and experiment for rectangular wave functions

We first examine the spectrum of frequency shifts produced by the sphere and pin perturbations for a given mode of the rectangular resonator. It is clear from Fig. 4 that a pin perturbation produces a more faithful image of the electric fields inside the microwave cavity. Let us now examine the degree to which the behavior of the pin and sphere perturbations agree with Slater's analysis. We consider the rectangular cavity mode images presented in Figs. 5 (pin perturbation) and 6 (sphere perturbation). The spectrum of frequency shifts for these images are shown in Fig. 4. The order of magnitude maximum frequency shift caused by a spherical perturbation in a previously uniform electric field is given by Eq. (4) and the radius of the sphere given above. For the TM_{170} mode shown in Fig. 6, the theoretical result is

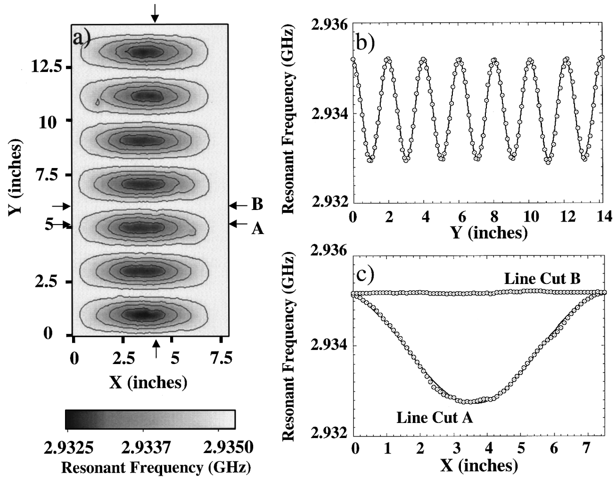

FIG. 5. (a) Measured frequency shift vs pin perturbation location in a TM_{170} mode of a rectangular microwave resonator. Also shown are (b) vertical and (c) horizontal line cuts through the data and comparisons to the theoretical frequency shifts.

$[(\omega_{\min}^2-\omega_0^2)/\omega_0^2]=-2.86\times10^{-4}$, which should be compared to the experimental value $[(\omega_{\min}^2-\omega_0^2)/\omega_0^2]=-7.78\times10^{-4}$. The magnetic field perturbation is predicted to produce a frequency shift of $[(\omega_{\max}^2-\omega_0^2)/\omega_0^2]=1.32\times10^{-4}$ versus an observed value of $[(\omega_{\max}^2-\omega_0^2)/\omega_0^2]=2.05\times10^{-4}$. In both cases, the predicted frequency shifts are approximately a factor of 2 lower than the observed values. Seen another way, the ratio of maximum electric to maximum magnetic perturbation is predicted to be approximately 2.2, whereas we observe a ratio of about 3.8. One reason for these discrepancies is that this calculation assumes the sphere is placed into an initially uniform electric field (i.e., in the middle of a parallel-plate capacitor with a plate separation much greater than the perturbation diameter). However, in our measurement the sphere lies in contact with one plate of the parallel-plate capacitor, thus significantly altering the field and producing a larger perturbation.

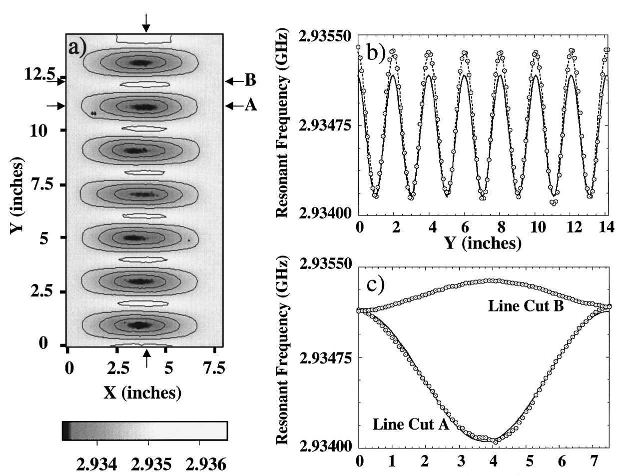

FIG. 6. (a) Measured frequency shift vs sphere perturbation location in a TM_{170} mode of a rectangular microwave resonator. Also shown are (b) vertical and (c) horizontal line cuts through the data and comparisons to the theoretical frequency shifts. In (b) the dashed line is a fit to a sinusoidal and the solid line a fit to a squared sinusoidal deviation from the resonant frequency.

For the pin perturbation, the data are in less agreement with theory, although they are in a favorable direction for electric field imaging. For the TM_{170} mode shown in Fig. 5, the electric field perturbation is predicted[1] to be $[(\omega_{\min}^2-\omega_0^2)/\omega_0^2]=-3.30\times10^{-4}$, compared to the experimental value $[(\omega_{\min}^2-\omega_0^2)/\omega_0^2]=-1.8\times10^{-3}$. The magnetic field perturbation is predicted to produce a frequency shift of $[(\omega_{\max}^2-\omega_0^2)/\omega_0^2]=1.04\times10^{-5}$ versus an observed value of $[(\omega_{\max}^2-\omega_0^2)/\omega_0^2]=4.9\times10^{-5}$. The ratio of maximum electric to maximum magnetic perturbation is predicted to be approximately 32, whereas we observe a ratio of about 37, again indicating a stronger perturbation which favors the electric fields. The reason for these discrepancies may again be due to the fact that the pin is in electrical contact with one of the walls of the resonator. We speculate that there is a ''lightning rod'' effect between the top of the pin and the top lid of the cavity which gives rise to enhanced electric field perturbation with no additional contribution from the magnetic field perturbation.

The rectangular cavity images in Figs. 5 and 6 show the resonant frequency of the cavity as a function of the position of the perturbation. The pin image (Fig. 5) shows a distribution which closely resembles the electric field amplitude squared distribution in a TM_{170} standing wave of a rectangular resonator. The sphere image, on the other hand, shows an additional feature which is due to contribution of the magnetic fields.

Line cuts of the data are shown on the sides of Figs. 5 and 6. The upper line cut (b) is a vertical cut through the seven main features, while the lower line cuts (c) are horizontal cuts through the data. Also shown in these line cuts are the expected theoretical frequency shifts based on solutions to the Helmholtz equation, calculated from Slater's formulas and scaled to fit the dynamic range of the data. The vertical line cut in the pin image [Fig. 5(b)] shows excellent agreement with the expected sinusoidal modulation of the resonant frequency. However, because of the additional magnetic field contributions, the vertical line cut of the sphere image [Fig. 6(b)] can also be fit to a simple sinusoidal modulation which incorrectly overestimates the probability amplitude [dashed line fit in Fig. 6(b)]. In this case, to extract just the electric field variation, one must identify the unperturbed resonant frequency in Fig. 4(a), and fit to a sinusoidal squared deviation from that frequency [solid line fit in Fig. 6(b)]. Likewise, the horizontal line cut of the pin image [Fig. 5(c), line cut A] shows a simple sinusoidal modulation through the peak and no measurable modulation between the peaks (line cut B). The corresponding horizontal line cuts of the sphere image [Fig. 6(c)] show sinusoidal modulation from electric field contribution (downward deviation) and magnetic field contributions (upward deviation). This analysis shows that the pin perturbation imaging method effectively eliminates contributions from magnetic fields in the standing wave images of our microwave resonator.

B. Wave chaotic cavity images

Shown in Figs. 7, 8, and 9 are probability amplitude $|\Psi_n|^2A$ images made with a pin perturbation of the bowtie resonator at 3.46, 5.37, and 11.94 GHz.[19] Here A is the area

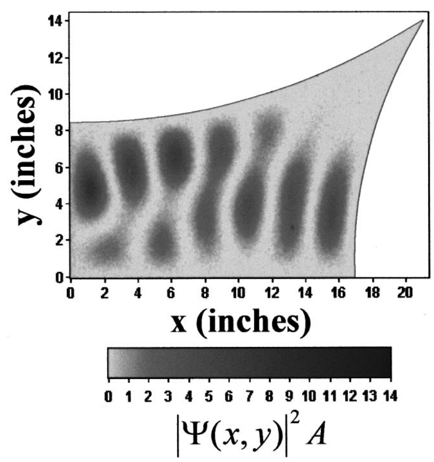

FIG. 7. Measured probability amplitude $|\Psi_n|^2 A$ in the quarter bowtie cavity, where A is the area of the entire cavity. This image is obtained from a resonant mode at 3.46 GHz.

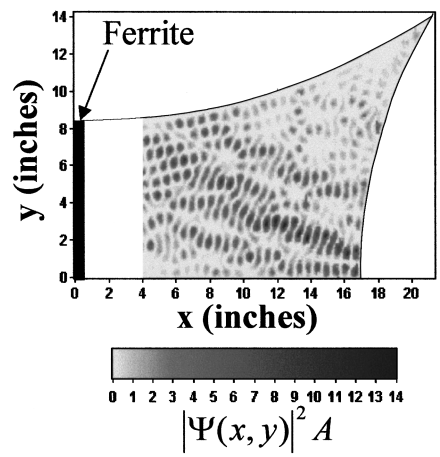

FIG. 9. Measured probability amplitude $|\Psi_n|^2 A$ in the quarter bowtie cavity, where A is the area of the entire cavity. This image is obtained from a resonant mode at 11.94 GHz. A ferrite bar is located along the left wall, as shown in Fig. 2.

of the cavity, $\int|\Psi_n|^2 dA=1$, and the frequency shifts above the unperturbed value are redefined to be zero in the plots. The field distributions in the chaotic eigenmode images are rather complicated and intricate. Although the patterns seem to be irregular, the probability amplitude maxima often form local regions with circular and linear structures. The linear structures, like those in Fig. 9, were noted by Heller *et al.* in wave functions produced by a random superposition of planes waves of fixed momentum.[15] Heller also noted the semicircular congregations of local maxima which surround regions of low probability amplitude, like those evident in Figs. 8 and 9, in random superpositions of plane waves. His explanation was that regions of low probability amplitude must be the source of radial nodes in the wave function, giving rise to semicircular clusters of high probability amplitude in the immediate surroundings.[15]

The low frequency modes shown in Figs. 5, 6, and 7 give us an opportunity to investigate the noise present in our images. From analysis of rectangular eigenfunctions where the wave functions are known, we can measure the signal-to-noise ratio (SNR) of the images. The SNR is defined as

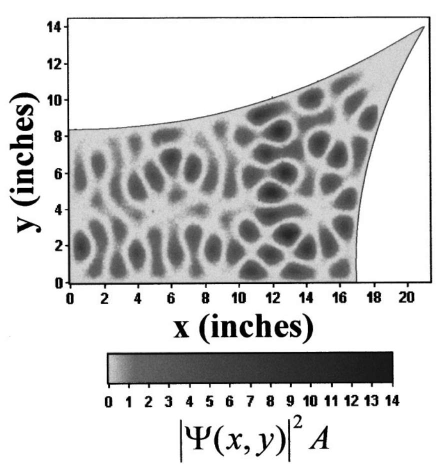

FIG. 8. Measured probability amplitude $|\Psi_n|^2 A$ in the quarter bowtie cavity, where A is the area of the entire cavity. This image is obtained from a resonant mode at 5.37 GHz.

the ratio of the frequency shift variation to the root mean square deviation between the predicted and observed frequency shift for a rectangular wave function. We find that the SNR is in the range of 30–60 at high input powers (+20 dBm from the amplifier) and does not degrade significantly even at the lowest source powers we used (−18 dBm). We thus have a very robust and clear method of imaging eigenfunctions.

The mode shown in Fig. 9 has features which are on the order of 0.5 in. in size. We find that features as small as 0.25 in. can be resolved by our imaging technique. The highest frequency mode imaged to date is at 15.4 GHz, where the guided wavelength in the resonator is approximately 1 in. In principle one could image at even higher frequencies, however the density of modes becomes too great to image without mode mixing.

A detailed analysis of the chaotic eigenfunctions is done through statistical analysis of their properties. The probability amplitude distribution function and the two-point correlation function of the eigenfunctions are important properties which are sensitive to the integrability of the potential well and the presence or absence of time-reversal symmetry. These properties are discussed in detail elsewhere.[10,20]

C. Background subtraction

When imaging broken time-reversal symmetry eigenstates with a ferrite present in the cavity, the scanning magnets have a slight effect on the ferrite due to the variable magnetic flux seen by the ferrite. This causes a background shift in the resonant frequency of the cavity mainly dependent on the scanning magnet location on the x axis (Fig. 1). The effect of the scanning magnet is minimized at the last point on the top right corner of the resonator (see Figs. 1 and 9). The electric field amplitude is zero on the boundaries, and the pin perturbation does not shift the resonant frequency of the cavity on the locations closest to the boundaries. Since this is the case, the shift in the resonant frequency along the boundaries is purely a function of the scanning magnet perturbation on the ferrite. Since the ferrite is placed along the y

axis on left side of the cavity, the effect of the scanning magnets is nearly constant as the magnet is moved in the y direction. Using this, we can subtract the difference between the last point in every y-axis column and the last point on the top right corner from the data in that column. This produces a flat background, leading to much cleaner images. The image shown in Fig. 9 has had a background subtracted, while those in the other figures have not.

V. LIMITATIONS AND CONSTRAINTS

We have several limitations on our measurements, including the resolution of the images, resonant frequency to be imaged, and the perturbation size. Eigenmode images are also affected by the perturbation caused by the coupling probes. These issues are discussed in Sec. V. Overall, the limitations on the measurements are significantly reduced by the choice of the perturbation and the method to scan the perturbation. Our imaging technique works in a remarkably broad frequency range from 700 MHz to about 15 GHz, where the upper limit is imposed by the density of eigenenergies for the cavity shown in Fig. 1.

A. Spatial resolution

To improve the spatial resolution of the images, particularly at high frequencies, we must use smaller perturbations. However, perturbations that are too small yield frequency shifts comparable to the uncertainty in the cavity resonant frequency due to noise (about 1 part in 10^3 of the 3 dB bandwidth). Very small perturbations may also fail to follow the magnet during the scan because they get stuck at the boundaries due to friction and surface tension of the lubricant used in the cavity.

We observe that spheres with a diameter less than 3/32 in. produce such a small perturbation that the noise in the system is the dominant factor in the eigenmode images. The smallest cylindrical pin which yields clear and complete images has a diameter of 0.0085 in. and a height of 0.1535 in. This pin is used for the 9–15.4 GHz frequency range images shown in this article (see Fig. 9).

B. Mode mixing

Since the field strengths at a given point in the cavity are different for different modes, shifts in the resonant frequencies due to a given perturbation are different. This can result in resonant frequencies which closely approach or cross over each other as the perturbation is scanned. For higher frequencies, where the mode density is higher, smaller perturbations must be used to avoid mode mixing.

Our technique for imaging the eigenfunctions of the hollow microwave cavity shown in Fig. 1 has high accuracy and success for frequencies up to 15.4 GHz. This limit can be pushed up, for instance, by using a silver layer on the inner walls of the cavity to increase the quality factor of the resonant modes. This would make it possible to clearly distinguish higher frequency modes from each other. In that case we can make use of smaller perturbations since smaller shifts in the resonant frequency of the cavity would be observable. For a typical bandwidth of 6.5 MHz for resonant frequencies above 10 GHz, the mode separation has to be on the order of 15 MHz to get reliable eigenmode images.

C. Perturbation movement

Another limit on the spatial resolution of our images is imposed by the perturbation movement mechanism. The stepper motors pull the magnet carriage with belts, and this mechanism imposes a lower limit for step size. The belts pulling the carriage carrying the magnets have backlash, and the stepper motors occasionally miss steps. The smallest step size we can use is 0.05 in. (using smaller step sizes will cause the scans to take more than 100 h). Returning the x–y stage to its home position on the y axis after each scan line minimizes the errors due to backlash and the errors caused by the missed steps.

The accuracy in perturbation location depends on the strength and the focus of the magnetic field used to drag the perturbation, as well as on the separation of the magnet from the perturbation. The friction between the perturbation and the cavity bottom surface while it is being dragged by the magnet can have a significant effect on the image quality. The friction is reduced by putting a thin layer of lubricant on the cavity floor. We find experimentally that the approximate standard deviation in the location of the pin is 0.025 in., about half the smallest step size used in the measurements (0.05 in.).

When the pin fails to follow the magnet, and either moves a little bit more or less than the magnet, the pin tilts due to the high divergence of the dc field of the scanner magnet. This tilt of the pin increases the magnetic field contribution to the frequency shift. The tilt of the pin is due to friction and can be minimized by moving it 0.1 in. more than where it is supposed to go and immediately drawing it back 0.1 in. We have found that for the pins with rough ends, the measured contribution to the frequency shift of the magnetic field components can exceed 20%. However for pins with smooth ends, the measured magnetic field contribution is on the order of 10%.

D. Coupling probe perturbation

The coupling ports perturb the cavity, resulting in a small change in the eigenfunction patterns. It has been observed that the coupling probe perturbation may even produce wave chaos in an integrable potential.[21] In order to measure the effect of the coupling on our images, a single bowtie resonator mode (Fig. 7) was imaged at three different coupling strengths. The coupling strength was varied by pulling the coupling probes out of the cavity. There was no visible change in the structure of the eigenfunction images, although the signal-to-noise ratio was degraded as the coupling was reduced.

VI. DISCUSSION

Our technique has successfully imaged the standing wave patterns of two-dimensional microwave resonators with and without time-reversal symmetry based on the simple physical principles of cavity perturbation. This technique allows us to image the eigenfunctions of a two-dimensional microwave cavity analog of the Schrödinger equation. Any hollow cavity (where E_z is not z dependent) can be mounted to the scanning setup and imaged. Since the magnet is scanned outside the cavity, there is no need to put holes on the cavity and change the boundaries other than at the coupling ports. Our experimental setup allows us to make high quality, high resolution images between 700 MHz and 15.4 GHz for a 1150 cm^2 area cavity.[19]

Our images show that we have avoided mode mixing and reduced the rf magnetic field contribution to an insignificant level. In addition, the data we have obtained using this technique are in qualitative agreement with the theoretical predictions made for the statistics of the field distribution. The technique can be used in similar cases where the amplitude of the electric field is the important quantity or eigenfunctions of the Schrödinger equation are needed for complicated quantum structures with hard wall boundary conditions.

ACKNOWLEDGMENTS

The authors would like to acknowledge assistance from Paul So, Edward Ott, Allen Smith and Tom Antonsen. This work was sponsored by the National Science Foundation through NSF NYI Grant No. DMR-92588183 and NSF Grant No. DMR-9624021.

[1] L. C. Maier, Jr. and J. C. Slater, J. Appl. Phys. **23**, 68 (1952).
[2] T. P. Budka, S. D. Waclawik, and G. M. Rebeiz, IEEE Trans. Microwave Theory Tech. **44**, 2174 (1996).
[3] A. Thanawalla, S. K. Dutta, C. P. Vlahacos, D. E. Steinhauer, B. J. Feenstra, S. M. Anlage, F. C. Wellstood, and R. H. Hammond, Appl. Phys. Lett. (submitted).
[4] A. S. Hou, F. Ho, and D. M. Bloom, Electron. Lett. **28**, 2302 (1992).
[5] D. W. van der Weide and P. Neuzil, J. Vac. Sci. Technol. B **14**, 4144 (1996).
[6] S. M. Anlage, C. P. Vlahacos, S. K. Dutta, and F. C. Wellstood, IEEE Trans. Appl. Supercond. **7**, 3686 (1997).
[7] S. Sridhar, Phys. Rev. Lett. **67**, 785 (1991).
[8] S. Sridhar, D. O. Hogenboom, and B. A. Willemsen, J. Stat. Phys. **68**, 239 (1992).
[9] J. Stein and H.-J. Stöckmann, Phys. Rev. Lett. **68**, 2867 (1992).
[10] D. H. Wu, A. Gokirmak, J. S. A. Bridgewater, and S. M. Anlage, Phys. Rev. Lett. (submitted).
[11] J. J. Hupert and G. Ott, Am. J. Phys. **34**, 260 (1966).
[12] J. J. Hupert, IRE Trans. Circuit Theory **CT-9**, 425 (1962).
[13] P. So, S. M. Anlage, E. Ott, and R. N. Oerter, Phys. Rev. Lett. **74**, 2662 (1995).
[14] T. M. Antonsen, Jr., E. Ott, Q. Chen, and R. N. Oerter, Phys. Rev. E **51**, 111 (1995).
[15] E. J. Heller, P. W. O'Connor, and J. Gehlen, Phys. Scr. **40**, 354 (1989).
[16] The scanning system consists of a XY-30 scanner, and the MD-2b dual stepper motor driver obtained from Arrick Robotics of Hurst, Texas.
[17] P. So, Ph.D. thesis, University of Maryland, 1996.
[18] The ferrite was obtained from TransTech of Adamstown, Maryland. It is model No. CVG1850, with a saturation magnetization of 1850 Oe, a resonance linewidth of 15 Oe, a dielectric constant of approximately 14.8, and dielectric loss tangent of less than 0.0002.
[19] Color images of these and other wave chaotic eigenfunctions are available at http://www.csr.umd.edu/research/hifreq/mw_cav.html.
[20] V. N. Prigodin, N. Taniguchi, A. Kudrollli, V. Kidambi, and S. Sridhar, Phys. Rev. Lett. **75**, 2392 (1995).
[21] F. Haake, G. Lenz, P. Seba, J. Stein, H.-J. Stockmann, and K. Zyczkowski, Phys. Rev. A **44**, R6161 (1991).